Author Manuscript
Author Manuscript
Author Manuscript
Author Manuscript

HHS Public Access
Author manuscript
Anal Chem. Author manuscript; available in PMC 2018 December 28.

Published in final edited form as:
Anal Chem. 2018 November 06; 90(21): 13036–13043. doi:10.1021/acs.analchem.8b04019.

Acetone/Isopropanol Photoinitiating System Enables Tunable Disulfide Reduction and Disulfide Mapping via Tandem Mass Spectrometry

Sarju Adhikari[†,‡], **Xiaoyue Yang**[†], and **Yu Xia**[*,†,‡]

[†] Department of Chemistry, MOE Key Laboratory of Bioorganic Phosphorus Chemistry and Chemical Biology, Tsinghua University, Beijing 100084, China

[‡] Department of Chemistry, Purdue University, West Lafayette, Indiana 47906, United States

Abstract

Herein, we report the development of a new photochemical system which enables rapid and tunable disulfide bond reduction and its application in disulfide mapping via online coupling with mass spectrometry (MS). Acetone, a clean and electrospray ionization (ESI) compatible solvent, is used as the photoinitiator (1% volume) in the solvent system consisting of 1:1 alkyl alcohol and water. Under ultraviolet (UV) irradiation (~254 nm), the acetone/alcohol system produces hydroxyalkyl radicals, which are responsible for disulfide bond cleavage in peptides. Acetone/isopropanol is most suitable for optimizing the disulfide reduction products, leading to almost complete conversion in less than 5 s when the reaction is conducted in a flow microreactor. The flow microreactor device not only facilitates direct coupling with ESI-MS but also allows fine-tuning of the extent of disulfide reduction by varying the UV exposure time. Near full sequence coverage for peptides consisting of intra- or interchain disulfide bonds has been achieved from complete disulfide reduction and online tandem mass spectrometry (MS/MS) via low energy collision-induced dissociation. Coupling different degrees of partial disulfide reduction with ESI-MS/MS allows disulfide mapping as demonstrated for characterizing the three disulfide bonds in insulin.

Graphical Abstract

[*]**Corresponding Author:** xiayu@mail.tsinghua.edu.cn.

Author Contributions
All authors have given approval to the final version of the manuscript

Notes
The authors declare no competing financial interest.

ASSOCIATED CONTENT
Supporting Information
The Supporting Information is available free of charge on the ACS Publications website at DOI: 10.1021/acs.analchem.8b04019.
Procedure for isotopic deconvolution and mass spectra data on disulfide bond cleavage using acetone/alcohol photoinitiating system (PDF)

Author Manuscript Author Manuscript Author Manuscript Author Manuscript

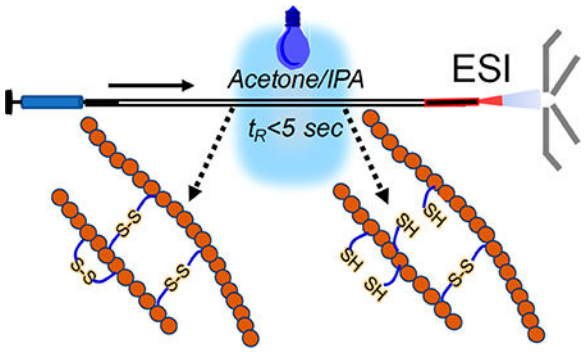

As mass spectrometry (MS) becomes the tool of choice for characterizing structural modifications in proteins, disulfide mapping still presents a challenge for current proteomics analysis workflows.[1] The issue is directly linked to the nature of gas-phase fragmentation chemistry of protonated peptide ions under low-energy collision-induced dissociation (CID), the most available tandem mass spectrometry (MS/MS) technique equipped on commercial mass spectrometers. As depicted by the mobile proton model,[2] disulfide bond does not dissociate readily as compared to the amide bonds under low-energy CID, often leading to no detectable sequence fragment ions for the backbone region inside a disulfide loop.[3] This aspect not only limits protein sequencing but also causes difficulty in disulfide mapping. To tackle this problem, disulfide bond reduction followed by alkylation[4] has been employed as a routine sample preparation procedure in bottom-up proteomics workflows.[5] Along this line, fast disulfide cleavage via chemical or electrochemical reduction has been developed which could be coupled with online liquid chromatography−mass spectrometry (LC−MS).[6,7] Besides, disulfide cleavage inside—the ionization source region has been demonstrated using electrospray ionization (ESI),[8–10] matrix-assisted laser desorption ionization (MALDI),[11] and reactive electrospray-assisted laser desorption/ionization (ELDI).[12] All above approaches when coupled with subsequent MS/MS (typically low-energy CID) deliver rich sequence information due to opening the disulfide bridges; however, disulfide linkage information is lost if complete disulfide reduction is adopted.

Alternative ion activation methods have been explored aiming to induce disulfide cleavages in the gas phase so that intact disulfide bonds can be preserved before MS analysis. Disulfide bond can be preferentially cleaved by electrons (in electron capture dissociation (ECD)[13,14] and electron transfer dissociation (ETD)[15]), photons (in 157 nm,[16] 266 nm,[17,18] and 193 nm ultraviolet photodissociation (UVPD)[19]), radicals (radical initiated peptide sequencing (FRIPS) and TEMPO conjugated peptide ions),[20] and oxidants in ion/ion reactions.[21] These methods can each be used as a stand-alone MS/MS technique or to be combined with CID to improve sequence coverage.

Disulfide mapping strategies rely heavily on multi-enzymatic digestion and partial disulfide reduction, with a goal to produce peptide digests only consisting of interchain disulfides. This type of structures is preferred since sequence fragments around cysteine amino acid residues associated with a disulfide bond are more likely to be generated from MS/MS, which is necessary for confident disulfide assignment. Such disulfide mapping approach has been recently demonstrated for human serum albumin (17 disulfide bonds)[8] and

Author Manuscript Author Manuscript Author Manuscript Author Manuscript

serotransferrin (19 disulfide bonds).[19] Finding the right conditions for partial reduction and proteolytic cleavages while avoiding disulfide scrambling is critical for successful disulfide mapping.[16,22] The optimization process is typically achieved by trial-and-error and the conditions cannot be generalized for different protein systems. Obviously, new methods that could either improve digestion or partial disulfide reduction will greatly advance the overall process for disulfide mapping.

Disulfides are known to be highly reactive toward radicals and the dominant reaction channel is disulfide bond cleavage. Earlier efforts from our group have shown that radicals produced from gas discharge[23] or ultraviolet (UV) irradiation[9,10] can cleave disulfide bonds within peptides near or in an ESI emitter. However, disulfide cleavage efficiency is only moderate and often accompanied by side reactions due to the lack of control of the reaction kinetics. In this work, we have developed a new photochemical reaction system for achieving efficient and tunable disulfide bond cleavage at the second-time scale. In this system, acetone was used as a clean and MS compatible photoinitiator upon 254 nm UV irradiation, while secondary hydroxyalkyl radicals resulting from alcohol cosolvent were responsible for cleaving the disulfide bond (Scheme 1). This photochemical reaction system was hyphenated with infusion ESI via a flow microreactor. Structural analysis capability of this photochemical system was demonstrated by coupling complete or partial disulfide cleavage with online ESI-MS/MS via CID for peptides containing one or multiple disulfide bonds.

EXPERIMENTAL SECTION

Materials.

Oxidized glutathione, reduced glutathione, methanol (MeOH), ethanol (EtOH), isopropyl alcohol (IPA), acetone, acetonitrile (ACN), TPCK treated trypsin, oxytocin, insulin from the porcine pancreas, and ribonuclease B were purchased from Sigma-Aldrich (St. Louis, MO, USA). Somatostatin-14 and selectin binding peptide were purchased from Aladdin (Shanghai, China) and GL Biochem Ltd. (Shanghai, China), respectively. The single letter sequence and disulfide bond connecting pattern for each peptide are listed in Supporting Information, Table S-1. d_3-Methanol (CD_3OH, 99.5 atom % D) and d_6-acetone (CD_3COCD_3, 99.9 atom % D) were purchased from J&K Scientific Ltd. (Beijing, China). All commercially purchased chemicals were used without further purification. Deionized water was obtained from a water purification system at 0.03 μS cm (Thermo Scientific; San Jose, CA, USA).

Peptide/Protein Digestion and Liquid Chromatography.

Trypsin digestion was conducted by mixing 10 μL of protein/peptide solution (10 μg/mL) with 15 μL of 20 mM ammonium acetate buffer, 5 μL acetonitrile, and 2 μL of trypsin (1 μg/μL), followed by incubation at 37 °C for 3 h. The trypsin digest was separated on a reversed phase LC (Shimadzu Corporation, Columbia, MD, USA). Column dimension was 4.6 mm × 150 mm with 5 μm C-18 packing material. Separation conditions for the digest are 0.1% formic acid in water (solvent A) and 0.1% formic acid in ACN (solvent B) with a linear gradient starting from 0% to 40% solvent B for 30 min at 0.5 mL/min flow rate.

Author Manuscript Author Manuscript Author Manuscript Author Manuscript

Photochemical Reactions in NanoESI Emitter and in Flow Microreactor.

A low-pressure mercury (LP-Hg) lamp with an emission band around 254 nm (BHK, Inc., Ontario, CA) was utilized to initiate the photochemical reactions. For the nanoESI setup, the lamp was placed orthogonally to the tip and off-axis by approximately 2−4 cm of the borosilicate glass emitter, as reported previously.[9] The flow microreactor was made from UV-transparently coated fused silica capillary (100 μm i.d., 375 μm o.d.; Polymicro Technologies; Phoenix, AZ).[24,25] The lamp was placed in parallel to the capillary (~10 cm exposure length) at 0.5 cm distance. The peptide solution was pumped through the microreactor (1−10 μL/min), the end of which was connected to the inlet of an infusion ESI source. All photochemical reaction setups were enclosed in a cardboard box to prevent direct human exposure to UV light.

Mass Spectrometry.

QTRAP 4000 and 4500 hybrid triple quadrupole/linear ion trap MS (SCIEX, Concord, ON, Canada) were used to perform preliminary studies with nanoESI emitter reaction setup. For the online coupling of the flow microreactor with infusion ESI-MS/MS, X500R TOF (SCIEX) was used. TIMS TOF (Bruker, Germany) was used to study partially disulfide reduced insulin products.

RESULTS AND DISCUSSION

Acetone/Alkyl Alcohol Photoinitiating System for Disulfide Cleavage.

Previously, our lab reported the use of hydroxyl radicals ($^{\bullet}$OH) for initiating hydroxyalkyl radical formation inside a nanoESI emitter, where alcohol was used as a cosolvent for nanoESI of disulfide peptides.[9] Disulfide cleavage was the main reaction channel; however, the reaction yield was limited due to relatively low concentrations of primary radicals ($^{\bullet}$OH) formed from 185 nm UV photolysis of ambient air.[9,26] An obvious way to improve the reaction yield is to use more efficient radical initiators, such as 2,2-dimethoxy-2-phenylacetophenone (DMPA) and benzophenone, which are commonly used in organic synthesis and radical polymerization.[27] These compounds go through Norrish type I cleavage at the α-carbon of the carbonyl group and form primary radicals for radical initiation upon UV irradiation.[28,29] They, however, are not directly compatible with MS analysis due to nonvolatile nature and relatively high concentrations (in millimolar) typically employed in the reaction system, which would cause severe interference to MS analysis. Acetone is the simplest ketone and it breaks down to acetyl radical and methyl radical upon UV irradiation (Scheme 1).[30,31] Considering that acetone has relatively low boiling point, low proton affinity, and it is miscible with most ESI solvent systems for peptide analysis, acetone should be well suited to be used as a photoinitiator.

To test the idea, 1% acetone (volume%) was added to an aqueous solution of oxidized glutathione (10 μM) and loaded onto the nanoESI reaction setup (Figure S1, Supporting Information). Before UV irradiation, only doubly protonated peptide ions ($[M + 2H]^{2+}$) at *m/z* 307.2 was observed (Figure 1a). After the lamp was turned on for about 2 min, intact peptide ions completely disappeared and new peaks resulting from disulfide bond cleavage dominated (Figure 1b). The major products are reduced glutathione ($[\gamma ECG + H]^{+}$, *m/z*

Author Manuscript Author Manuscript Author Manuscript Author Manuscript

308.0) and radical substitution products at cysteinyl sulfur, including methyl radical ($^{\bullet}CH_3$, *m/z* 322.1), acetyl radical ($^{\bullet}C(O)CH_3$, *m/z* 350.1), and acetonyl radical ($^{\bullet}CH_2C(O)\text{-}CH_3$, *m/z* 361.1), respectively. The identity of these products were verified by accurate mass measurements and MS/MS experiments. The same reaction was repeated without addition of acetone. No reaction products associated with disulfide bond cleavage were observed, even with prolonged UV exposure (~5 min). Homolytic cleavage of disulfide bond can be induced by 193−266 nm UV irradiation;[18,32] the absence of the disulfide cleavage without acetone addition in our study could be due to low photon flux of the UV lamp. The above set of experiments clearly suggests that Norrish Type I cleavage of acetone indeed happens for 1% of acetone upon 254 nm UV irradiation. Similar reaction phenomenon was observed with as low as 0.1% (v%) of acetone addition, albeit with longer UV irradiation time. Although disulfide bond cleavage is 100% by reacting with radicals derived from photolysis of acetone, the presence of multiple reaction channels points out the need to convert the first-generation radicals into less reactive secondary radical species. In this study, we focused on forming hydroxyalkyl radicals via using acetone as a photoinitiator.

Formation of hydroxyalkyl radicals was explored by adding alkyl alcohol precursor as cosolvent in the reaction system. Figure 1c shows the nanoESI spectrum of oxidized glutathione in MeOH/H_2O ((v/v) = 1:1, 1% acetone) solvent system upon UV irradiation. As a big contrast to Figure 1b where no methanol was added, only two distinct reaction products were observed, corresponding to the reduced (*m/z* 308.2) and *S*-hydroxymethyl modified glutathione ions (*m/z* 338.2). *S*-hydroxymethyl product was verified by detecting signature formaldehyde loss (30 Da) from low energy CID (Figure S2, Supporting Information).[9] The extracted ion chromatogram (XIC) showed that the intact glutathione had a sharp drop from 100% to 0% within 30 s (UV irradiation 1.1−1.5 min), accompanied by steep increase of the reduced peptide (*m/z* 308), the ion signal of which maximized at 1.2 min UV irradiation and then dropped to reach a steady state within 20 s. During this time, the ion signal of the hydroxymethyl substitution product (*m/z* 338) increased rapidly and stayed constant afterward. These kinetic data suggest that reduced thiol might be further converted to *S*-hydroxymethyl product after its initial formation. Indeed, almost identical spectrum to Figure 1c was obtained when the oxidized glutathione was replaced by reduced glutathione for the reaction (Figure S3, Supporting Information). No definitive evidence could be obtained for tracing the singly protonated thiyl radical ions since they overlap with the doubly protonated glutathione ions at *m/z* 307.2.

The reaction phenomena for solvent systems involving larger alkyl alcohols, viz. EtOH and IPA, were similar to that observed in the MeOH solvent system. That is, 100% disulfide cleavage was achieved and only two reaction products were detected (Figure 1e,f). MS^2 CID of the substitution products, *m/z* 352 (Figure 1e) and *m/z* 366 (Figure 1f) showed abundant loss of 44 and 58 Da, confirming the formation of the respective S-hydroxyalkyl product (Figure S2, Supporting Information). A distinct difference from the acetone/MeOH system is that the yield of reduced thiol was increased significantly from 32% (MeOH) to 80% (EtOH) and 93% (IPA).

The possible reaction pathways accounting for disulfide cleavage using acetone/alcohol photoinitiating system are proposed in Scheme 1. Direct disulfide/photon interactions are

Author Manuscript Author Manuscript Author Manuscript Author Manuscript

considered negligible due to low photon flux and orders of magnitude lower concentration of the peptide relative to acetone. The reaction pathway is likely to be initiated by photochemical decomposition of acetone into methyl/acetyl radicals.[30] In the presence of a large excess of alcohol, acetone should have little chance to interact with peptide directly, while reaction with alcohol solvent is the main reaction channel. In the case of methanol, the formation of hydroxymethyl radical ($^{\bullet}CH_2OH$) due to hydrogen abstraction from the C−H bond of methanol is supported by the D_3COH experiments (Figure S4, Supporting Information). For larger alcohols, hydrogen abstraction is generally preferred from the α-position due to its lower C−H bond dissociation energy.[33] For example, the BDE of C_α−H in $(CH_3)_2C$−HOH is 380.7 kJ/mol, while that of the C_β–H is 394.6 kJ/mol.[34]

Mechanistic studies involving reactions of hydroxyalkyl radicals with disulfides have been scarce.[33] Data generated from gas-phase reactions and theoretical calculations suggest that carbon-centered radicals cleave disulfide bond via a substitution mechanism.[35,36] Based on the observed products, we hypothesize that hydroxyalkyl radical attacks the disulfide bond, forming thiyl radical and S-hydroxyalkyl at the cleavage site. The thiyl radical can further abstract a hydrogen atom from hydroxyalkyl radical (BDE, ~150 kJ/mol for O−H in $^{\bullet}C(CH_3)_2OH$),[37] forming reduced thiol and aldehyde/ketone as stable products. Hydroxyalkyl radicals can also react with a reduced thiol to form S-hydroxyalkyl product and the reactivity follows the order of $^{\bullet}CH_2OH$ > $^{\bullet}CH(CH_3)OH$ > $^{\bullet}C$-$(CH_3)_2OH$, as supported from reaction data of reduced glutathione. It is worth noting that the pathways described above are intended to describe the overall reaction phenomenon. Detailed mechanistic investigations are beyond the scope of the current report.

Disulfide Reduction in a Flow Microreactor.

Comparing the data for disulfide cleavage in Figure 1 using different alkyl alcohol as cosolvent, IPA solvent system stood out for producing reduced disulfide product with almost 100% conversion. Therefore, 1% acetone in 1:1 IPA/H_2O was chosen as the optimal solvent system for peptide and protein analysis. Previously, our group has demonstrated that photochemical reactions can be greatly accelerated relative to bulk reactions when conducted in a flow microreactor due to significantly improved photon efficiency using flow path in micrometer-dimension.[24,25] Flow microreactor is also advantageous regarding precise control of reaction time so as to reduce detrimental side-reactions from prolonged UV exposure as found by using a static nanoESI setup. UV-transparently coated fused silica capillary was employed to construct the flow microreactor, which was connected directly to an infusion ESI source for online MS experiments as shown in Figure 2a.

Such a reaction system was tested with a peptide containing an interchain disulfide bond (sequence shown the inset of Figure 2b). Figure 2b,c compares the ESI-MS spectra before and after UV irradiation in positive ion mode. Clearly, after 3 s UV irradiation, the intact peptide ions ($[M + 2H]^{2+}$, *m/z* 467.2) were 100% consumed, while ions corresponding to the two reduced peptide chains, $[A + H]^+$ (*m/z* 378.2) and $[B + H]^+$ (*m/z* 558.2), dominated in the postreaction spectrum. The progress of reduction was monitored as a function of the UV irradiation time. As shown in Figure 2d, the yield of disulfide reduction increases monotonically as UV irradiation time increases and it reaches 100% after 4 s. Above kinetic

Author Manuscript Author Manuscript Author Manuscript Author Manuscript

data demonstrate that the degree of disulfide bond reduction could be tuned by adjusting the UV exposure time of the peptide in the flow microreactor, which is particularly useful for achieving partial disulfide reduction for peptides containing multiple disulfide bonds.

Increasing Sequence Coverage for Disulfide Peptides and Proteins from Complete Reduction.

Selectin binding peptide is a naturally existing circular peptide due to an intrachain disulfide bond between C1 and C9 residues (sequence shown in the inset of Figure 3). As expected, no sequence ions were obtained from MS^2 CID of doubly protonated intact peptide ions (Figure S5, Supporting Information). After 5 s UV irradiation, 100% disulfide reduction was achieved for this peptide, as demonstrated by the complete disappearance of intact peptide ions ($[M + 2H]^{2+}$, *m/z* 523.8, Figure 3a) and appearance of ions at *m/z* 524.7 ($[^{red}M + 2H]^{2+}$) ions (Figure 3b). MS^2 CID of the reduced product at *m/z* 524.7 gave almost full series of b- and y-type fragment ions, allowing sequence identification of the peptide (Figure 3c). Similar reaction phenomenon was observed with another peptide containing intrachain disulfide bond (oxytocin, Figure S6, Supporting Information).

Lysozyme (four disulfide bonds, 129 amino acid residues) was tested as a model for larger proteins. Complete disulfide reduction of all four disulfide bonds were achieved within 5 s UV irradiation as compared to 3 h reduction using DTT. MS^2 CID of the reduced lysozyme ions (+15, *m/z* 955.1) produced rich backbone fragmentation for sequence identification (Figure S7, Supporting Information,).

We further applied complete disulfide reduction for the analysis of protein digests, mimicking the bottom-up proteomic approach. Ribonuclease-B, a small protein containing four disulfide bonds (sequence shown in Figure S8, Supporting Information) was subjected to trypsin digestion and LC separation before disulfide reduction and ESI-MS/MS analysis. One disulfide peptide was detected after digestion, which contained three peptide chains connected by two interchain disulfide bonds: C_{40}−C_{95} and C_{58}−C_{110} (sequence shown in Figure 4). The other predicted peptide containing C_{26}−C_{84} and C_{65}−C_{72} disulfide bonds was not detected, possibly due to its resistance to proteolytic digestion.[38] Figure 4a and 4b compare the ESI-MS spectra of the peptide before and after UV irradiation (5 s). Clearly, the intact peptide ions ($[M + 6H]^{6+}$, $[M + 5H]^{5+}$, $[M + 4H]^{3+}$) completely disappeared after UV irradiation. The presence of three separated peptide chains, viz. $[A + 3H]^{3+}$(*m/z* 802.1), $[B + H]^{+}$ (*m/z* 858.4), and $[C + 2H]^{2+}$ (*m/z* 1084.5), confirmed the presence of two interchain disulfide bonds in this peptide. The intact peptide ions ($[M + 6H]^{6+}$) and the disulfide reduced A, B, and C chains ($[A + 3H]^{3+}$, $[B + H]^{+}$, $[C + 2H]^{2+}$) were each subjected to MS^2 CID for structural analysis (spectra shown in Figure S9). The fragmentation map of the intact and reduced peptide ions is summarized in Figure 4c. MS^2 CID of the disulfide reduced chains led to almost 100% sequencing of the peptide, allowing determination of cysteine residues at C_{40} and C_{58} in A chain, C_{95} in B chain, and C_{110} in C chain. MS^2 CID of the intact peptide produced a series of sequence ions in A chain with intact B chain attached, i.e., BAb_2, BAb_9, BAb_{10}, BAb_{11}, BAb_{14}, BAb_{15}, BAb_{16}, and BAb_{17}, suggesting a disulfide linkage at C_{40}−C_{95}. Several fragment ions specific to the C chain were obtained,

Author Manuscript Author Manuscript Author Manuscript Author Manuscript

confirming its presence in the intact peptide, which could only be linked to A chain through a disulfide linkage at C_{58}−C_{110}.

Mapping Disulfide Bonds in Insulin from Tunable Partial Reduction.

A distinct advantage of the photochemical reaction system is the capability of tuning the degree of disulfide reduction simply by adjusting the UV irradiation time (in seconds). This tunability is critical in analyzing disulfide connecting patterns for intact proteins or peptides which contain multiple disulfide bonds. Such aspect is demonstrated by disulfide mapping of porcine insulin, which consists of two interchain disulfide linkages between chain A and chain B (AC_7−BC_7 and AC_{20}−BC_{19}) and one intrachain linkage within chain A (AC_6 −AC_{11}). Data in Figure 5 compare the ESI-MS spectra of insulin before UV and after different periods of UV irradiation. Before UV irradiation, the protonated insulin ions, 5+ and 4+ (*m/z* 1156.3 and 1145.3), dominated in the spectrum (Figure 5a). After 1.8 s UV irradiation, ions of A chain (3+ at *m/z* 795.3 and 2+ at *m/z* 1192.0) and B chain (4+ at *m/z* 850.9 and 3+ at *m/z* 1133.9) appeared as abundant species (Figure 5b). Deconvolution of the isotope cluster of the remaining insulin 5+ ions showed that it contained 53% intact, 31% and 16% one disulfide and two disulfide reduced species, respectively (Figure 5e, deconvolution procedure in Supporting Information). When the UV irradiation time was extended to 3.1 s, the remaining 5+ ion population only contained 12% intact insulin ions, while the one and two disulfides reduced species was 28% and 60%, respectively (Figure 5f). It is worth noting that partial disulfide reduction typically produced a mixture of different degrees of disulfide reduction; however, due to the capability of online reaction monitoring the optimized condition for a certain reduced population could be achieved rapidly. The intact 5+ insulin ions and those resulting from different degrees of reduction (1.8 and 3.1 s UV irradiation) were each subjected to MS^2 CID for disulfide mapping. The lower *m/z* region (500−900) of the CID data are summarized in Figure 6a–c and the corresponding fragmentation maps derived from detected b-and y-type ions are summarized in Figure 6d–f. CID data in the higher *m/z* region are supplied in the Figure S10, Supporting Information. As expected, MS^2 CID of the intact insulin ions (5+, *m/z* 1156.1, Figure 6a) only produced sequence fragment ions in the exocyclic backbone regions and no specific information regarding disulfide linkage can be obtained. However, MS^2CID of the fully reduced A^{2+} and B^{5+} ions produced full sequence coverage of each chain, allowing pinpointing the positions of the six cysteine residues (Figure S11, Supporting Information).

Figure 6b shows MS^2 CID of the 5+ ions (*m/z* 1156.5) containing 31% one disulfide reduced and 16% two disulfide reduced species. The presence of Bb_{7-18} ions suggests an interchain disulfide had been cleaved before CID and this bond should involve C_7 residue in chain B. On the other hand, the detection of $BAy_{4,\ 6-8}$ ions allow for locating an interchain disulfide bond between AC_{20} and BC_{19}. Two sequence ions were detected between AC_6 and AC_{11}, viz. Ab_6 and Ab_7, albeit at relatively low intensities (inset of Figure 6b). This phenomenon is suggestive for an intrachain disulfide in this sequence region. MS^2 CID of the 5+ insulin ions containing 60% two disulfides reduced species is shown in Figure 6c with unique ions highlighted in red. The presence of abundant Ab_{6-9} and BAy_{11-15} ions clearly suggests that this ion population contains structures with the intrachain disulfide bond in chain A and an interchain disulfide bond (AC_7−BC_7) had been reduced. It is worth

Author Manuscript Author Manuscript Author Manuscript Author Manuscript

mentioning that the relative ion intensities of Ab_6 and Ab_7 are significantly increased as the two disulfide reduced species increased from 16% to 60% (insets of Figure 6b,c), supporting that they are likely derived from the two-disulfide bond reduced population. Interestingly, no fragment ion relating to structures containing reduced AC_{20}−BC_{19} disulfide was observed. If this disulfide bond had been cleaved, sequence ions such as By_{12-23}, ABb_{7-17}, Ay_{1-10}, or BAb_{11-20} should be present. The above data clearly demonstrate that disulfide reduction was slowest for the disulfide bond between AC_{20}−BC_{19}. The difference in the disulfide reduction kinetics could be attributed to the different solvent accessibility of the three disulfide bonds, in which the AC_{20}−BC_{19} has been reported to be least accessible in insulin under electrochemical reduction.[39]

Although the two interchain disulfide bonds have been pinpointed from MS^2 CID of the partially reduced insulin ions, the intrachain disulfide bond in chain A still needs to be determined. To acquire such information, ions of partially reduced chain A (2+, *m/z* 1191.0) which consisted of an intact intrachain disulfide bond but with two other interchain disulfide bonds being cleaved, were subjected to MS^2 CID. It is worth pointing out that a small portion of the fully reduced A chain ions was inevitably mixed in the precursor ion population and underwent beam-type CID together with the partially reduced A chain ions even from using the narrowest isolation window available on the instrument. Nevertheless, comparisons of the CID data between the partially reduced and the fully reduced A chain ions showed that the relative ion intensities of b_{6-10} were significantly reduced from the partially reduced A chain ion population while those of exocyclic sequence ions were quite comparable, i.e., $b_{4,5}$ and b_{11-17} (data shown in Figure S12, Supporting Information). Consequently, the disulfide linkage between C_6 and C_{10} in chain A was determined.

CONCLUSIONS

A photochemical reaction system that allows for rapid and tunable disulfide reduction has been developed for characterizing peptides containing one or multiple disulfide bonds by ESI-MS/MS. Acetone/IPA is determined as the best photoinitiating system for disulfide bond reduction with almost 100% yield achieved within less than 5 s UV irradiation. The use of flow microreactor enables precise control of the degree of disulfide reduction and online coupling with infusion ESI-MS/MS. By pairing complete disulfide reduction with subsequent low-energy CID, near complete sequence coverage is achieved for various peptides containing one or multiple disulfide bonds. Furthermore, different degrees of partial reduction can be achieved simply by adjusting the UV irradiation time, greatly facilitating the disulfide linkage assignment, as demonstrated by mapping the three disulfide bonds in insulin. For the peptide systems studied herein, no evidence for disulfide bond scrambling has been obtained, likely benefited from the fast reaction and online detection system. Compared to conventional disulfide mapping approach, the online photochemical system enjoys several distinct advantages, including full compatibility with ESI-MS without introducing any chemical matrix, significantly shortened reaction time (from hours to seconds) and flexibility in tuning the extent of disulfide reduction. These aspects are highly desirable for developing high-throughput structural analysis capability for proteins consisting of multiple disulfide bonds. As a preliminary test, disulfide reduction in the microflow reactor was online-coupled with reversed phase LC−MS. Disulfide linkage

Author Manuscript Author Manuscript Author Manuscript Author Manuscript

analysis was successful for peptide digest of a model protein. Detailed characterization of this system for bottom-up protein analysis is currently undergoing and will be reported separately.

Supplementary Material

Refer to Web version on PubMed Central for supplementary material.

ACKNOWLEDGMENTS

Financial support from National Natural Science Foundation of China (Grant No. 21722506, Grant No. 21621003) and Grant NIH R01GM118484 is greatly appreciated. We acknowledge assistance from D. Zhang for isotope deconvolution.

REFERENCES

(1). Lakbub JC; Shipman JT; Desaire H *Anal. Bioanal. Chem*. 2018, 410, 2467–2484. [PubMed: 29256076]

(2). Wysocki VH; Tsaprailis G; Smith LL; Breci LA *J. Mass Spectrom*. 2000, 35, 1399–1406. [PubMed: 11180630]

(3). Lioe H; O'Hair RA *J. Am. Soc. Mass Spectrom*. 2007, 18, 1109–1123. [PubMed: 17462910]

(4). Wall JS *J. Agric. Food Chem*. 1971, 19, 619–625. [PubMed: 5163841]

(5). Zhang Y; Fonslow BR; Shan B; Baek M-C; Yates JR *Chem. Rev*. 2013, 113, 2343–2394. [PubMed: 23438204]

6). Zhang Y; Cui W; Zhang H; Dewald HD; Chen H *Anal. Chem*. 2012, 84, 3838–3842. [PubMed: 22448817]

(7). Mysling S; Salbo R; Ploug M; Jørgensen TJ D. *Anal. Chem*. 2014, 86, 340–345.

(8). Cramer CN; Kelstrup CD; Olsen JV; Haselmann KF; Nielsen PK *Anal. Chem*. 2017, 89, 5949–5957. [PubMed: 28453249]

(9). Stinson CA; Xia YJ *Am. Soc. Mass Spectrom*. 2014, 25, 1192–1201.

(10). Durand KL; Tan L; Stinson CA; Love-Nkansah CB; Ma X; Xia YJ *Am. Soc. Mass Spectrom*. 2017, 28, 1099–1108.

(11). Fukuyama Y; Iwamoto S; Tanaka KJ Mass Spectrom. 2006, 41, 191–201.

(12). Peng IX; Ogorzalek Loo RR; Shiea J; Loo JA *Anal. Chem*. 2008, 80, 6995–7003. [PubMed: 18683952]

(13). Zubarev RA; Kelleher NL; McLafferty FW *J. Am. Chem. Soc*. 1998, 120, 3265–3266.

(14). Oh H; Breuker K; Sze SK; Ge Y; Carpenter BK; McLafferty FW *Proc. Natl. Acad. Sci. U. S. A*. 2002, 99, 15863–15868. [PubMed: 12444260]

(15). Syka JEP; Coon JJ; Schroeder MJ; Shabanowitz J; Hunt DF *Proc. Natl. Acad. Sci. U. S. A*. 2004, 101, 9528–9533. [PubMed: 15210983]

(16). Foley SF; Sun Y; Zheng TS; Wen D *Anal. Biochem*. 2008, 377, 95–104. [PubMed: 18358819]

(17). Fung YME; Kjeldsen F; Silivra OA; Chan TWD; Zubarev RA *Angew. Chem*. 2005, 117, 6557–6561.

(18). Agarwal A; Diedrich JK; Julian RR *Anal. Chem*. 2011, 83, 6455–6458. [PubMed: 21797266]

(19). Quick MM; Crittenden CM; Rosenberg JA; Brodbelt JS *Anal. Chem*. 2018, 90, 8523–8530. [PubMed: 29902373]

(20). Lee M; Lee Y; Kang M; Park H; Seong Y; Sung BJ; Moon B; Oh HB *J. Mass Spectrom*. 2011, 46, 830–839. [PubMed: 21834022]

(21). Pilo AL; McLuckey SA *Anal. Chem*. 2016, 88, 8972–8979. [PubMed: 27531151]

(22). Gray WR Protein Sci. 1993, 2, 1732–1748. [PubMed: 8251945]

(23). Xia Y; Cooks RG *Anal. Chem*. 2010, 82, 2856–2864. [PubMed: 20196567]

Author Manuscript Author Manuscript Author Manuscript Author Manuscript

(24). Adhikari S; Xia Y *Anal. Chem*. 2017, 89, 12631–12635. [PubMed: 29155553]

(25). Adhikari S; Zhang W; Xie X; Chen Q; Xia Y *Anal. Chem*. 2018, 90, 5239–5246. [PubMed: 29570972]

(26). Creasey DJ; Heard DE; Lee JD *Geophys. Res. Lett*. 2000, 27, 1651–1654.

(27). Hoyle CE; Bowman CN *Angew. Chem., Int. Ed*. 2010, 49, 1540–1573.

(28). Norrish RGW; Kirkbride FW *J. Chem. Soc*. 1932, 1518–1530.

(29). Norrish RG Trans W. Faraday Soc. 1934, 30, 103–113.

(30). Norrish RGW; Crone HG; Saltmarsh OD J. Chem. Soc 1934, 1456–1464.

(31). Haas Y *Photochem. Photobiol. Sci*. 2004, 3, 6–16. [PubMed: 14743272]

(32). Bookwalter CW; Zoller DL; Ross PL; Johnston MV *J. Am. Soc. Mass Spectrom*. 1995, 6, 872–876. [PubMed: 24214431]

(33). Akhlaq MS; Murthy CP; Steenken S; Von Sonntag CJ *Phys. Chem*. 1989, 93, 4331–4334.

(34). Luo Y-R Handbook of Bond Dissociation Energies in Organic Compounds; CRC Press: Boca Raton, FL, 2003.

(35). Krenske EH; Pryor WA; Houk KN *J. Org. Chem*. 2009, 74, 5356–5360. [PubMed: 19548657]

(36). Anglada JM; Crehuet R; Adhikari S; Francisco JS; Xia Y *Phys. Chem. Chem. Phys*. 2018, 20, 4793–4804. [PubMed: 29383342]

(37). Internet Bond-energy Databank (pKa and BDE)-iBonD, http://ibond.chem.tsinghua.edu.cn, accessed July 2018.

(38). Bernard BA; Newton SA; Olden KJ *Biol. Chem*. 1983, 258, 12198–12202.

(39). Cramer CN; Haselmann KF; Olsen JV; Nielsen PK *Anal. Chem*. 2016, 88, 1585–1592. [PubMed: 26695097]

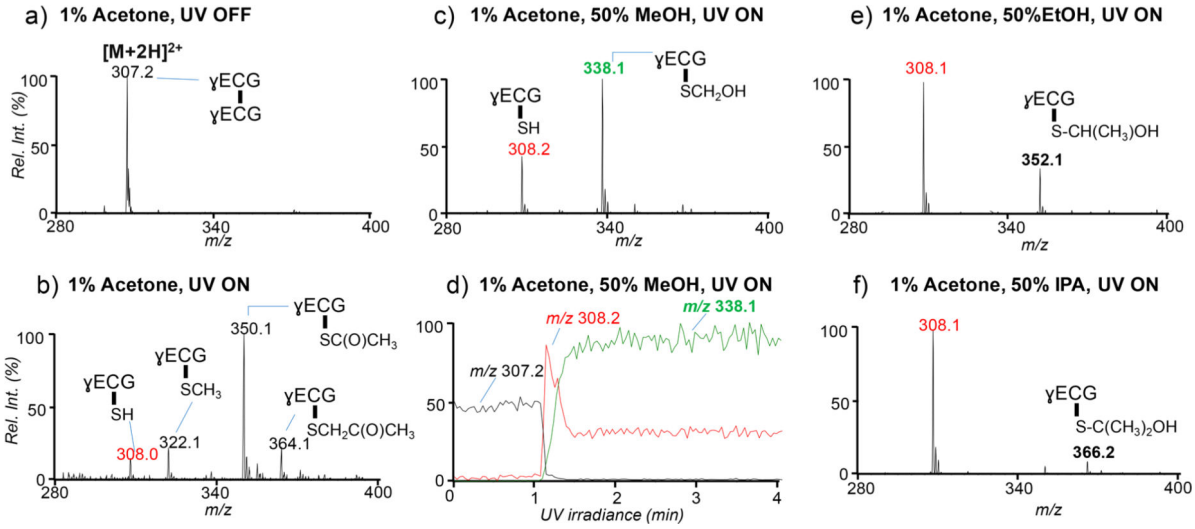

Figure 1.

Positive ion mode MS spectra of oxidized glutathione (10 μM) prepared in solutions containing 1% acetone as a photoinitiator. (a) Before and (b) after UV exposure of the aqueous solution in nanoESI emitter. (c) UV irradiation of the peptide in H_2O/MeOH ((v/v) = 1:1) and (d) extracted ion chromatogram (XIC) for the reaction shown in part c. UV irradiation of the peptide in (e) H_2O/EtOH ((v/v) = 1:1) and (f) H_2O/IPA ((v/v) = 1:1).

Author Manuscript Author Manuscript Author Manuscript Author Manuscript

Author Manuscript Author Manuscript Author Manuscript Author Manuscript

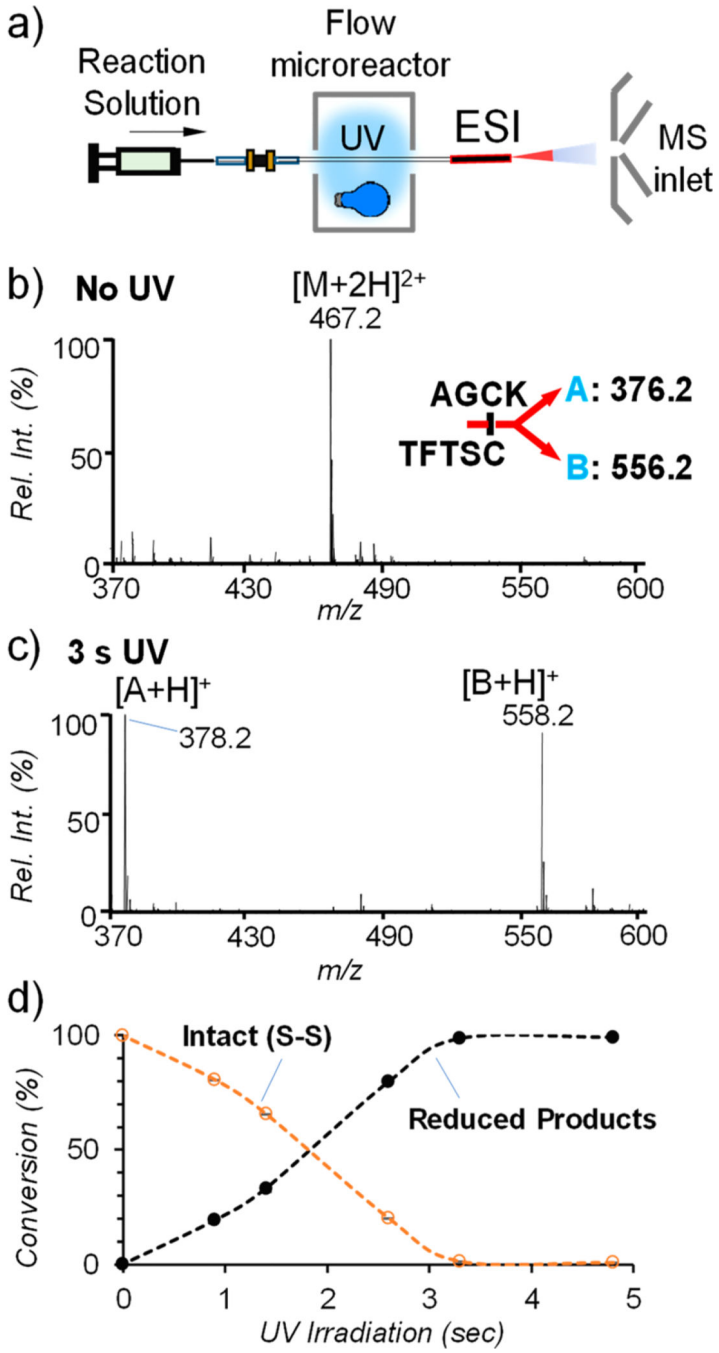

Figure 2.

(a) Flow microreactor setup for coupling acetone/IPA imitated disulfide bond reduction with ESI-MS. ESI-MS spectra of 10 μM of trypsin-digested somatostatin-14 in H_2O/IPA (1:1) with 1% acetone (b) before UV and (c) after 3 s UV irradiation in positive ion mode. d) Plot of % conversion of the intact peptide to disulfide reduced species as a function of UV irradiation time.

Author Manuscript Author Manuscript Author Manuscript Author Manuscript

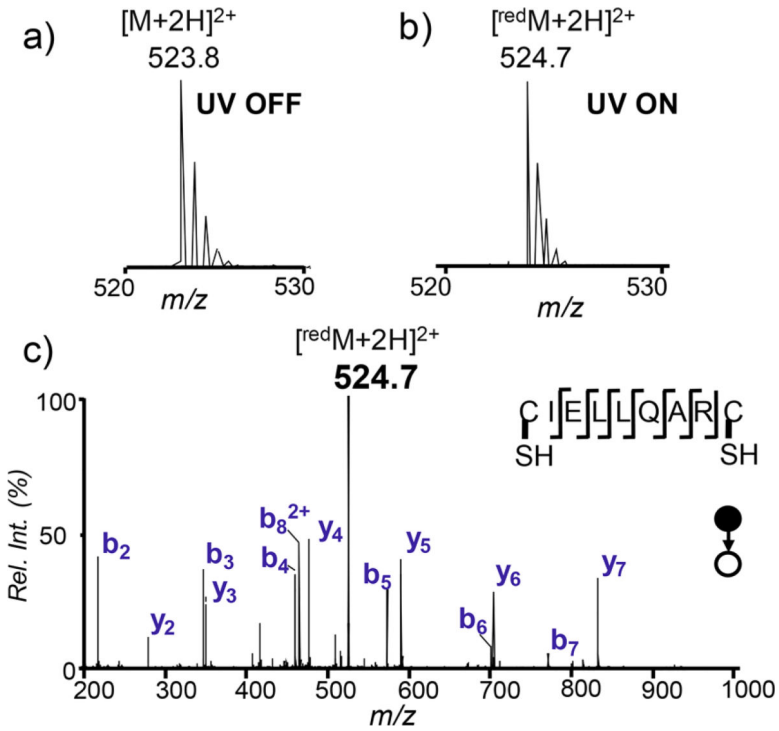

Figure 3.

MS spectra of 10 μM of selectin binding peptide dissolved in H_2O/IPA (1:1) with 1% acetone: (a) before UV, (b) after 5 s UV irradiation in flow microreactor, and (c) MS^2 CID of reduced peptide ions at *m/z* 524.7 ($[^{red}M + 2H]^{2+}$). The fragmentation map of the peptide is indicated in the inset.

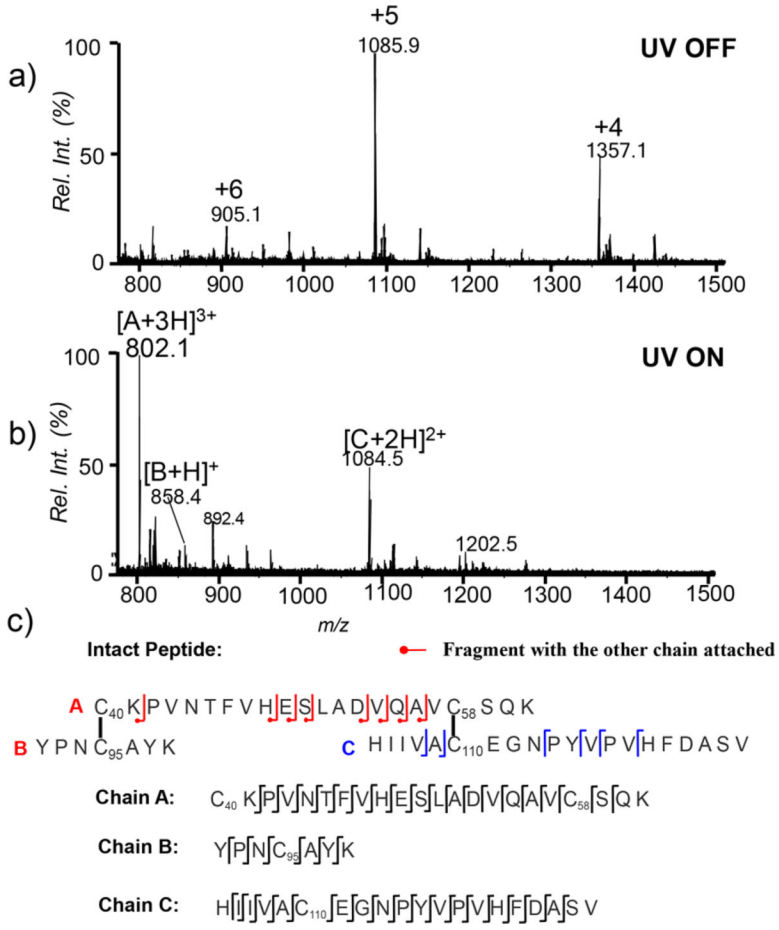

Figure 4.

MS spectra of trypsin-digested ribonuclease-B subjected to the radical reaction: (a) before UV and (b) after 5 s UV irradiation in flow microreactor. (c) Sequence and fragmentation maps of intact peptide and reduced A, B, and C chains.

Author Manuscript Author Manuscript Author Manuscript Author Manuscript

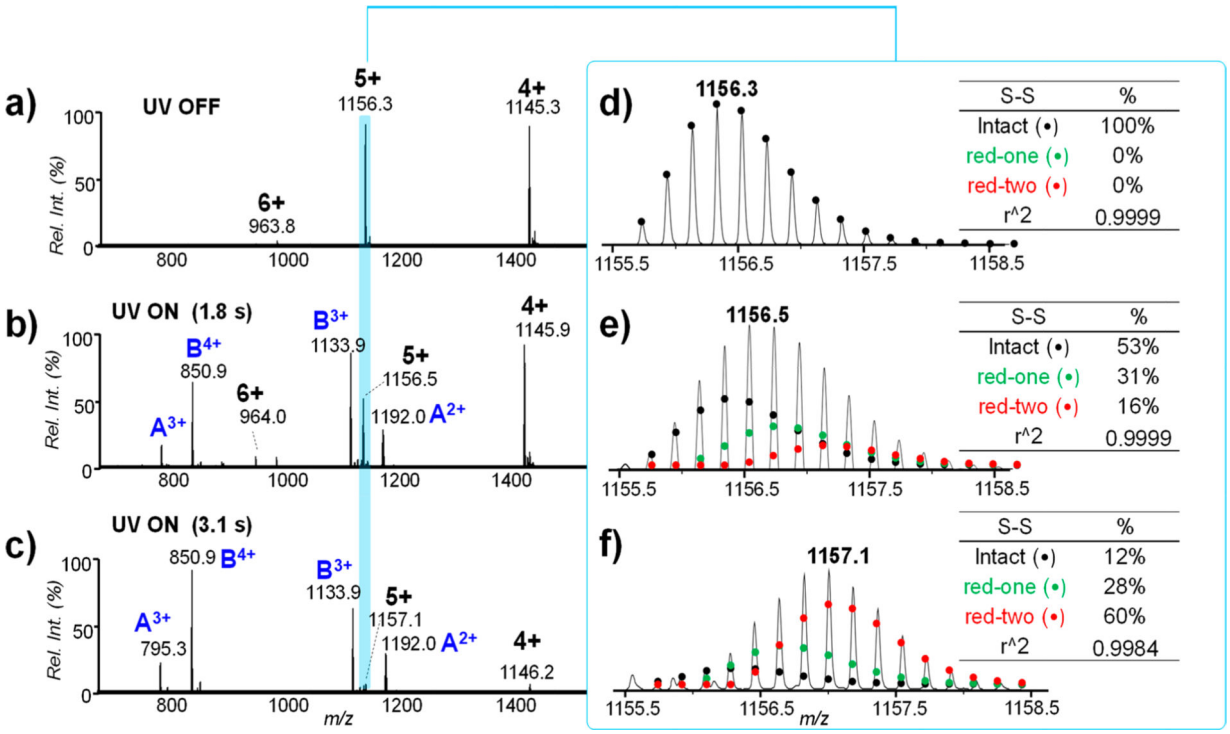

Figure 5.

Positive ion mode ESI MS spectra of porcine insulin in 1% acetone, IPA/H_2O ((v/v) = 1:1). (a) Before UV, (b) after 1.8 s, and (c) 3.1 s UV irradiation in flow microreactor. (d−f) The zoomed-in region of 5+ insulin ions from parts a−c. Deconvoluted isotopic distributions of the intact (black dots), one disulfide reduced (green dots), and two disulfide reduced (red dots) species are overlaid with the experimental data and their relative contributions are listed in the insets.

Author Manuscript Author Manuscript Author Manuscript Author Manuscript

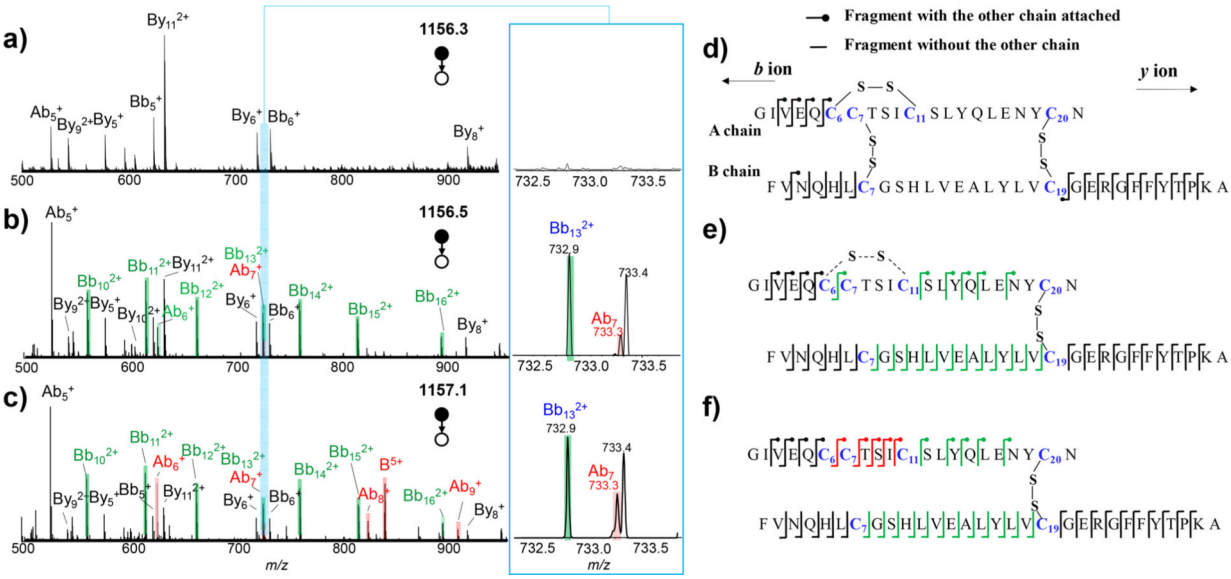

Figure 6.

MS^2 CID of 5+ insulin ion populations derived from (a) intact, (b) 31% one disulfide reduced and 16% two disulfide reduced species, and (c) 28% one disulfide reduced and 60% two disulfide reduced species. The corresponding fragmentation maps are shown in parts d −f.

Author Manuscript Author Manuscript Author Manuscript Author Manuscript

Author Manuscript Author Manuscript Author Manuscript Author Manuscript

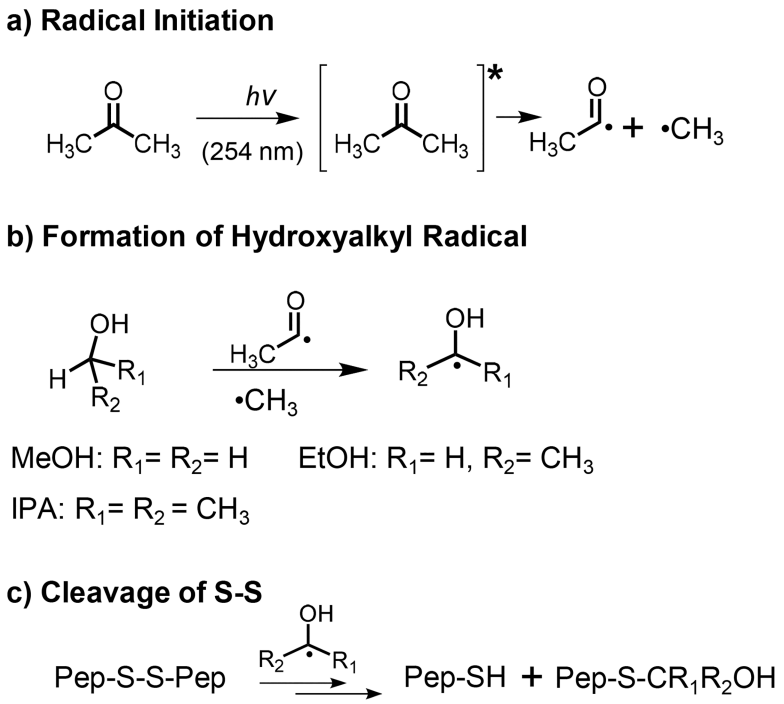

Scheme 1.

Proposed Reaction Pathways for Disulfide Bond Cleavage from Using Acetone/Alkyl Alcohol Photoinitiating System